

Shift of responsive peak in GaN-based metal-insulator-semiconductor photodetectors

Kun You, Hong Jiang, Dabing Li, Xiaojuan Sun, Hang Song et al.

Citation: *Appl. Phys. Lett.* **100**, 121109 (2012); doi: 10.1063/1.3696025

View online: <http://dx.doi.org/10.1063/1.3696025>

View Table of Contents: <http://apl.aip.org/resource/1/APPLAB/v100/i12>

Published by the [American Institute of Physics](#).

Related Articles

Tuning the dynamic properties of electrons between a quantum well and quantum dots

J. Appl. Phys. **112**, 043702 (2012)

High responsivity near-infrared photodetectors in evaporated Ge-on-Si

Appl. Phys. Lett. **101**, 081101 (2012)

Dual-color ultraviolet photodetector based on mixed-phase-MgZnO/i-MgO/p-Si double heterojunction

Appl. Phys. Lett. **101**, 081104 (2012)

Enhanced performance of photodetector and photovoltaic based on carrier reflector and back surface field generated by doped graphene

Appl. Phys. Lett. **101**, 073906 (2012)

Gallium free type II InAs/InAs_xSb_{1-x} superlattice photodetectors

Appl. Phys. Lett. **101**, 071111 (2012)

Additional information on *Appl. Phys. Lett.*

Journal Homepage: <http://apl.aip.org/>

Journal Information: http://apl.aip.org/about/about_the_journal

Top downloads: http://apl.aip.org/features/most_downloaded

Information for Authors: <http://apl.aip.org/authors>

ADVERTISEMENT



HAVE YOU HEARD?

Employers hiring scientists
and engineers trust
physicstodayJOBS



<http://careers.physicstoday.org/post.cfm>

Shift of responsive peak in GaN-based metal-insulator-semiconductor photodetectors

Kun You,^{1,2} Hong Jiang,^{1,a)} Dabing Li,¹ Xiaojuan Sun,^{1,2} Hang Song,¹ Yiren Chen,^{1,2} Zhiming Li,¹ Guoqing Miao,¹ and Hongbo Liu¹

¹State Key Laboratory of Luminescence and Applications, Changchun Institute of Optics, Fine Mechanics and Physics, Chinese Academy of Sciences, Changchun 130033, People's Republic of China

²Graduate School of the Chinese Academy of Sciences, Beijing 100039, People's Republic of China

(Received 6 January 2012; accepted 1 March 2012; published online 21 March 2012)

A gallium nitride (GaN)-based metal-insulator-semiconductor (MIS) ultraviolet photodetector (PD) was fabricated on a sapphire substrate. It was found that the responsive peak of the GaN-based MIS PD redshifted with increasing negative bias, which has not been reported before. Also, the shift of the responsive peak has been interpreted in terms of the tunneling procedure of the photo-generated holes assisted by defects in the interfaces between the GaN layers and the SiN_x layers. © 2012 American Institute of Physics. [<http://dx.doi.org/10.1063/1.3696025>]

Gallium nitride (GaN) is considered to be one of the most promising materials for the development of high responsivity and visible blind ultraviolet (UV) photodetectors (PDs) because of its wide direct band gap (~ 3.4 eV). This wide band gap allows instruments using GaN UV PDs to operate in an environment with significant visible and infrared radiation without expensive visible and infrared blocking filters. Also, the high saturation velocity ($v_s = 2.7 \times 10^7$ cm/s)¹ of GaN leads to high photocurrent and high responsivity for the GaN PDs.

Recently, many GaN-based UV PDs have been reported, including a photoconductive PD,^{2,3} a metal-semiconductor (MS) junction PD,⁴ a p-n junction PD,⁵ a p-i-n PD (Ref. 6), and avalanche photodiodes.⁷ Unfortunately, in highly Mg doped GaN, compensation effects lead to a decrease in the free hole concentration.⁸ It is therefore difficult to further improve the performance of the p-n junction PD, p-i-n PD, and avalanche photodiodes. Also, when compared with the photoconductive PD, the MS PDs have many attractive advantages for practical applications, such as low capacitance, high speed, simplicity of fabrication, and compatibility with field effect transistor technology,^{9–11} which make MS PDs the most promising candidates for high-speed photodetection applications. To achieve good performance in MS UV PDs, it is important to improve the crystal quality and obtain a large Schottky barrier height at the MS interface, leading to small leakage currents and high breakdown voltages, which result in improvements in responsivity and photocurrent to dark current contrast ratio. To achieve the large Schottky barrier height on GaN, one method is to use metals with high work functions between the metal and semiconductor.¹² However, many of the high work function metals are not sufficiently stable. Also, severe interdiffusion occurs at the metal-GaN interface. To solve this problem, we can insert an insulating layer between the metal and the underlying semiconductor.¹³ With this insulating layer, we can also effectively suppress the leakage current of the PDs.

In this paper, we report the fabrication of GaN-based metal-insulator-semiconductor (MIS) UV PDs. The optical and electrical properties of the fabricated PDs are also discussed.

The GaN samples were prepared in a horizontal metal organic chemical vapor deposition reactor operating at 70 Torr. Trimethylgallium and ammonia gases were used as the precursor chemicals with hydrogen gas as the carrier. Silane (SiH₄) was used as the dopant source gas. The substrate used was (0 0 0 1)-oriented sapphire. Immediately before growth, the substrate surfaces were prepared by *in situ* thermal treatment at 1100 °C for 5 min. A ~ 25 -nm-thick nucleation layer was deposited at 550 °C, followed by a 2.5- μ m undoped GaN layer at 1050 °C. A 1.2- μ m Si-doped GaN layer was then deposited on top of the sample at 1050 °C. From room temperature Hall measurements, it was found that the electron concentration was 2.2×10^{18} cm⁻³. Room temperature photoluminescence (PL) and x-ray diffraction (XRD) measurements were also performed to evaluate the quality of the as-grown samples.

The GaN MIS PDs were then fabricated. First, the GaN samples were cleaned using acetone and alcohol, and then SiN_x was deposited on top of the samples by magnetron sputtering. The target was silicon with a purity of 99.95%, and the distance between the target and the substrate was 5.5 cm. The background pressure in the sputtering chamber was 2.8×10^{-4} Pa. The deposition processes were performed in an Ar (15 sccm) and N₂ (30 sccm) ambient, which was controlled using a mass flow meter at an applied RF power of 150 W. The working pressure was maintained at 0.7 Pa. The thickness of the SiN_x layer was measured to be ~ 10 nm by scanning electron microscopy. To determine the atomic fractions of the SiN_x layer, we deposited the same SiN_x film on a GaAs substrate at the same time. Energy dispersive spectroscopy (EDS) was then used to determine the atomic fractions of the SiN_x film.

After SiN_x deposition, the sample was cleaned with acetone and alcohol and dried using purified N₂. Finally, we deposited a 100-nm Al layer on the surface of the samples by thermal evaporation to serve as the metal contacts. The contacts were 1 mm \times 1 mm in size, and the sensitive area of the

^{a)} Author to whom correspondence should be addressed. Electronic mail: jiangh@ciomp.ac.cn.

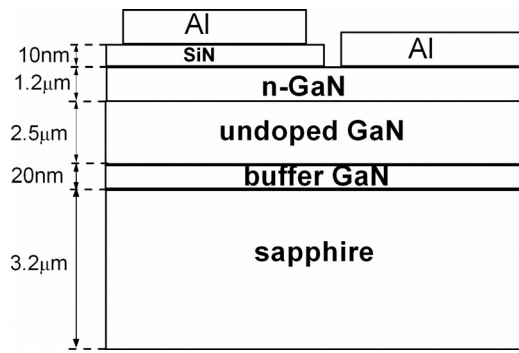


FIG. 1. Schematic of the GaN MIS photodetectors.

detector was 0.1 mm^2 . The schematic structures of the MIS PDs fabricated in this study are shown in Fig. 1.

Room temperature current-voltage (I-V) characteristics of the devices were then measured using a Keithley 237 source meter unit under dark conditions. The photoresponse characteristics of the device were measured using a standard lock-in technique using a 150 W Xe lamp as the excitation light source.

Fig. 2 shows the measured XRD pattern of the GaN epitaxial film prepared on the sapphire substrate. The peak located at $2\theta = 41.9^\circ$ in the pattern originated from the (0 0 6) plane of the sapphire substrate. We also observed a GaN (0 0 2) XRD peak at $2\theta = 34.7^\circ$ with a full width at half maximum (FWHM) of 0.079° . This result indicates that the GaN film is grown in the c-axis direction with good crystal quality. The inset of Fig. 2 shows the room temperature PL spectrum of our GaN epitaxial films. It was found that a strong PL peak existed at 367.5 nm (3.37 eV) with a FWHM of the PL peak of only 37 meV. All of these results indicated the good crystal quality of our GaN epitaxial layers.

The EDS results for the deposited SiN_x film are shown in Fig. 3. From the EDS, it was found that the N/Si atom ratio of the SiN_x is 1.32, which is below that of stoichiometric Si_3N_4 . This indicated that N vacancies exist in the SiN_x films.

When a bias is applied to the GaN side, the I-V characteristics (Fig. 4(a)) show good rectifying behavior with a rectification ratio ($I_{\text{forward}}/I_{\text{reverse}}$) of more than 5.5×10^2 at 4 V in the dark, which indicates the formation of a diode. The

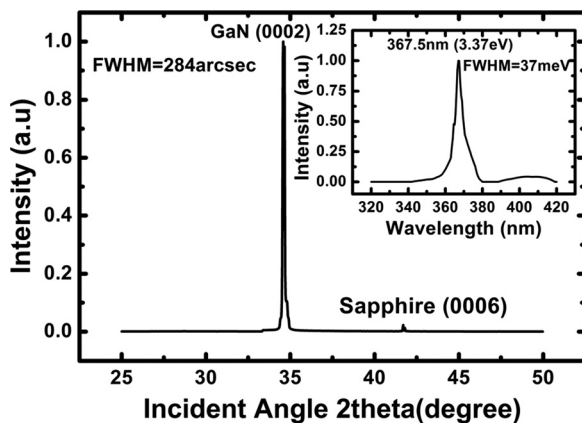
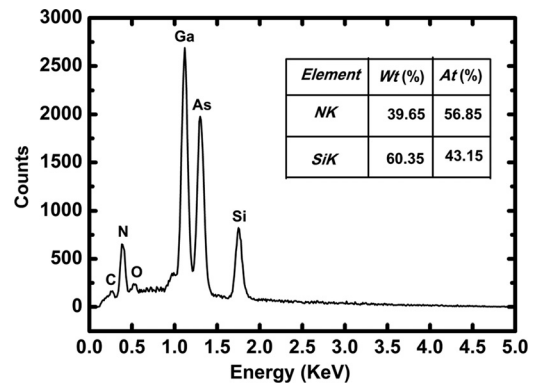


FIG. 2. XRD pattern and PL spectrum of the GaN film grown on a sapphire substrate. The inset shows the room temperature PL spectrum of the GaN films.

FIG. 3. EDS results for the SiN_x film on a GaAs substrate.

high rectification ratio indicates the high quality of the electrical properties of our sample device. The turn-on voltage, the reverse leakage current, and the zero bias resistance are found to be 0.5 V, $2.1 \times 10^{-8} \text{ A}$ at -0.5 V , and $1.79 \times 10^8 \Omega$, respectively, by fitting of the I-V characteristics according to the method detailed in Ref. 14. The negative current of the GaN MIS PD is shown in black in Fig. 4(b), and it is found that the negative current increases exponentially according to the equation, $I \propto \exp(\alpha V)$, which is usually observed in wide band gap p-n diodes because of the recombination-tunneling mechanism^{15,16}. The constant α is found to be 1.14 V^{-1} from fitting of the experimental data in Fig. 4(b), as shown in red, which is within the range of $0.45\text{--}1.50 \text{ V}^{-1}$ for the semiconductor junctions, as suggested by Fedison *et al.*¹⁷ Also, the I-V characteristics between the two as-deposited Al contacts on GaN are linear, indicating the formation of ohmic contacts (see the inset of Fig. 4(a)).

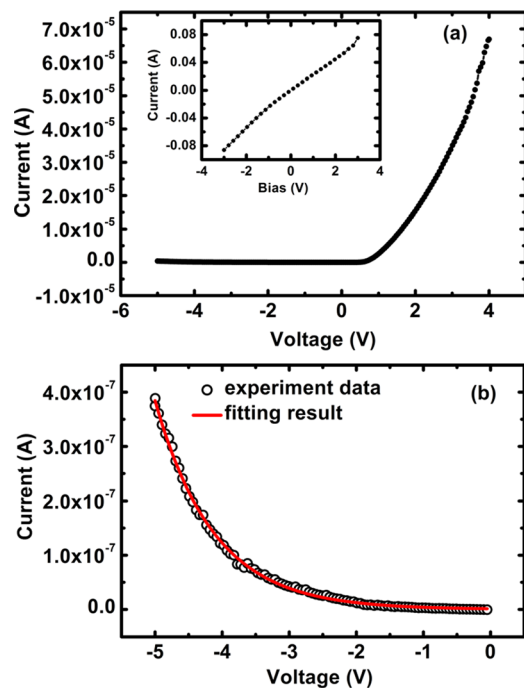


FIG. 4. (Color online) (a) I-V curves of the GaN MIS PDs, while the inset shows I-V characteristics between two aluminum contacts on the GaN films and (b) the I-V characteristics of the GaN MIS PD under negative bias (circle), while the solid line shows the fitting results.

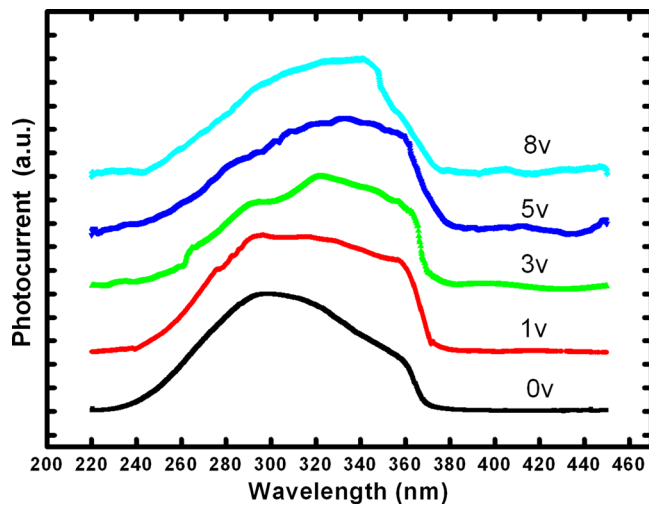


FIG. 5. (Color online) Photocurrent spectra of GaN MIS detectors when applying 0 V, 1 V, 3 V, 5 V, and 8 V negative bias.

The photocurrent spectrum of the GaN MIS PD when irradiated from the SiN_x side under the application of various negative bias levels is shown in Fig. 5. From this spectrum, we found that at 0 V bias, the GaN-based MIS PD produces a response. By increasing the bias, the response at longer wavelengths is enhanced. As a result, the wavelength of the photocurrent peak is redshifted along with the increasing negative bias. Under negative bias values of 0 V, 1 V, 3 V, 5 V, and 8 V, the wavelengths of the photocurrent peaks were found to be 298 nm, 298 nm, 325 nm, 340 nm, and 343 nm, respectively, and the photocurrent peaks were found to be 13.3 nA, 20.7 nA, 173.3 nA, 533.3 nA, and 906.6 nA, respectively.

This phenomenon can be explained by the tunneling of the photo-generated holes assisted by the traps at the interfaces. It is well known that when the sample is exposed to light, many electron-hole pairs will be generated in the GaN layer. Under the reverse electrical field of the barrier, the electrons are driven towards the negative electrode (GaN side), and the holes are driven towards the positive electrode (SiN_x side). However, because of the high density of the traps at the interface between GaN and SiN_x , the holes cannot tunnel through the SiN_x barrier easily and are captured by the trap energy levels. According to the quantum mechanism, when the bias is low, only holes with higher energy can tunnel through the barrier easily. As a result, when the bias is low, the photoresponse at shorter wavelengths will be greater. When the bias increases, the effective barrier height decreases, and thus holes with lower energies can also tunnel through the barrier. Consequently, the photoresponse at longer wavelengths is enhanced when the bias increases. In other words, the hole tunneling probability follows the equation:

$$T = D_0 \exp \left\{ -\frac{4\pi}{h} \int_a^b \sqrt{2m[V(x) - E]} dx \right\}, \quad (1)$$

where $V(x)$, E , m , and D_0 are the one-dimensional potential barrier, the particle energy, the particle mass, and a normalized coefficient, respectively. From Eq. (1), the tunneling probability is seen to be modulated by the potential barrier

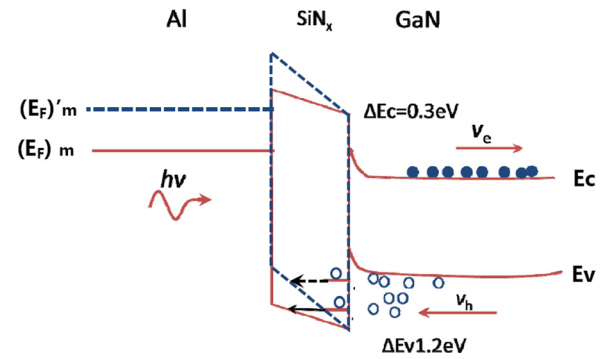


FIG. 6. (Color online) Energy band diagram for the GaN MIS detectors under a small negative bias (solid line) and under increased negative bias (dashed line).

and the particle energy, which in turn is modulated by the bias and the trap depth at the interface between GaN and SiN_x .

To further illustrate this tunneling process, the energy diagram of the GaN MIS detector for different negative bias levels is shown in Fig. 6. The ΔE_v between GaN and Si_3N_4 has been measured to be 1.2 eV using x-ray photoelectron spectroscopy.¹⁸ Also, Gritsenko *et al.*¹⁹ and Aozasa *et al.*²⁰ have proved the existence of the defect energy level trap 2 (t2), which is caused by an N atom vacancy and an H atom (from the residual atmosphere in the vacuum chamber) in the Si_3N_4 film, and is approximately 0.8 eV above the valence band. Robertson *et al.* have proved the existence of the defect energy level trap 1 (t1), which is caused by Si-Si defects in the Si_3N_4 and is approximately 0.3 eV above the valence band.²¹ When the samples are illuminated, the photo-generated holes in the interfaces will be captured by trap 1 and trap 2. When the negative bias is low (0 V, 1 V), only the holes trapped in trap 1 can tunnel through the barrier (solid line in Fig. 6), which corresponds to the photocurrent peak at 295 nm. When the negative bias increased (3 V), the height of the barrier decreased. As a result, the holes trapped in both trap 1 and trap 2 can both tunnel through the barrier (dashed line in Fig. 6), which corresponds to the photocurrent peak at 325 nm. When the negative bias increases further (5 V and 8 V), the barrier is narrow enough to allow the holes in the valence band to tunnel through, which corresponds to the photocurrent peak at 340 nm. In this case, the photocurrent spectrum showed the intrinsic energy band characteristics of GaN films.

In conclusion, GaN MIS UV PDs were fabricated. The dark current and optical responsivity were measured and analyzed. EDS results indicated that N vacancies existed in the SiN_x layer, and the I - V curve showed that tunneling mechanics assisted by the defects dominated the current transport procedure in the devices. A shift in the responsive peak wavelength phenomenon has been observed and explained using the tunneling assisted by the defect energy levels in the insulator layer.

This work was partly supported by the National Key Basic Research Program of China (Grant No. 2011CB301901), the National Natural Science Foundation of China (Grant Nos. 51072196 and 51072195), and the National High-Tech R&D Program (863, Grant No. 2011AA03A111).

- ¹T. Sawada, Y. Ito, K. Imai, K. Suzuki, H. Tomozawa, and S. Sakai, *Appl. Surf. Sci.* **159**, 449 (2000).
- ²S. Han, W. Jin, D. Zhang, T. Tang, C. Li, X. Liu, Z. Liu, B. Lei, and C. Zhou, *Chem. Phys. Lett.* **389**, 176 (2004).
- ³B. W. Lim, Q. C. Chen, J. Y. Yang, and M. Asif Khan, *Appl. Phys. Lett.* **68**, 3761 (1996).
- ⁴Q. Chen, J. W. Yang, A. Osinsky, S. Gangopadhyay, B. Lim, and M. Z. Anwar, *Appl. Phys. Lett.* **70**, 2277 (1997).
- ⁵R. Hickman, J. M. Van Hove, P. P. Chow, J. J. Klaassen, A. M. Wowchak, C. J. Polley, D. J. King, F. Ren, C. R. Abernathy, S. J. Pearton *et al.*, *Solid-State Electron.* **44**, 377 (2000).
- ⁶Y. Kang, Y. Xu, D. Zhao, and J. Fang, *Solid-State Electron.* **49**, 1135 (2005).
- ⁷D. Yoo, J. Limb, J.-H. Ryou, Y. Zhang, S.-C. Shen, R. D. Dupuis, D. Hanser, E. Preble, and K. Evans, *IEEE Photon. Technol. Lett.* **19**, 1313 (2007).
- ⁸P. Vennegues, M. Benaissa, S. Dalmasso, M. Leroux, E. Feltin, P. De Mierry, B. Beaumont, B. Damilano, N. Grandjean, and P. Gibart, *Mater. Sci. Eng., B* **93**, 224 (2002).
- ⁹R. P. Joshi, A. N. Dharamsi, and J. McAdoo, *Appl. Phys. Lett.* **64**, 3611 (1994).
- ¹⁰E. Monroy, F. Calle, J. L. Pau, E. Munoz, F. Omnes, B. Beaumont, and P. Gibart, *Phys. Status Solidi A* **185**, 91 (2001).
- ¹¹J. C. Carrano, T. Li, P. A. Grudowski, C. J. Eiting, R. D. Dupuis, and J. C. Campbell, *J. Appl. Phys.* **83**, 6148 (1998).
- ¹²F. D. Auret, S. A. Goodman, M. Hayes, M. J. Legodi, H. A. van Laarhoven, and D. C. Look, *Appl. Phys. Lett.* **79**, 3074 (2001).
- ¹³A. Chini, J. Wittich, S. Heikman, S. Keller, S. P. DenBaars, and U. K. Mishra, *IEEE Electron Device Lett.* **25**, 55 (2004).
- ¹⁴S. Zeyrek, S. Altindal, H. Yuzer, and M. M. Bulbul, *Appl. Surf. Sci.* **252**, 2999 (2006).
- ¹⁵L. J. Mandalapu, F. X. Xiu, Z. Yang, D. T. Zhao, and J. L. Liu, *Appl. Phys. Lett.* **88**, 112108 (2006).
- ¹⁶R. Ghosh and D. Basak, *Appl. Phys. Lett.* **90**, 243106 (2007).
- ¹⁷J. B. Fedison, T. P. Chow, H. Lu, and I. B. Bhat, *Appl. Phys. Lett.* **72**, 2841 (1998).
- ¹⁸R. Nakasaki, T. Hashizume, and H. Hasegawa, *Physica. E* **7**, 953 (2000).
- ¹⁹V. A. Gritsenko, S. S. Nekrashevich, V. V. Vasilev, and A. V. Shaposhnikov, *Microelectron. Eng.* **86**, 1866 (2009).
- ²⁰H. Aozasa, I. Fujiwara, A. Nakamura, and Y. Komatsu, *Jpn. J. Appl. Phys.* **38**, 1441 (1999).
- ²¹J. Robertson and M. J. Powell, *Appl. Phys. Lett.* **44**, 415 (1984).